ARTICLES

Molecular and Solid-State Modeling of the Crystal Purity and Morphology of ϵ-Caprolactam in the Presence of Synthesis Impurities and the Imino-Tautomeric Species Caprolactim

Patricia Mougin[†]

Centre of Molecular and Interface Engineering, School of Engineering and Physical Sciences, Heriot-Watt University, Riccarton, Edinburgh EH14 4AS, U.K.

Graham Clydesdale, Robert B. Hammond,* and Kevin J. Roberts

Institute of Particle Science and Engineering, Department of Chemical Engineering, University of Leeds, Leeds LS2 9JT, U.K.

Received: February 11, 2003; In Final Form: September 28, 2003

A study of impurity incorporation into host crystal surfaces, using molecular modeling techniques, is presented for ϵ-caprolactam, illustrating a rapid method for predicting the effects of additives on the purity and shape of particles formed through crystallization. Optimum positions, in terms of calculated lattice energy, were located for the impurity molecules within the host crystal lattice. Differential binding energies and modified attachment energies were calculated using the program HABIT95 (Clydesdale, G.; Roberts, K. J; Docherty, R. *Quantum Chemistry Program Exchange* **1996**, *16*, 1) for each impurity molecule for all the important growth forms. From the differential binding energies, values were calculated for the equilibrium segregation coefficients. The impact of the impurities cyclohexane, cyclohexanol, cyclohexanone, and the imino-tautomeric form of ϵ-caprolactam (or caprolactim) was considered in the study. Excellent agreement was found between calculated equilibrium segregation coefficients for the impurity cyclohexanone in the {110} and {11$\bar{1}$} forms of ϵ-caprolactam and reported experimental values for crystals grown from the melt in the presence of a wide range of cyclohexanone impurity concentrations, 0.1−30 mol %, for supersaturations of the melt, 2×10^{-3} to 6×10^{-3} (van den Berg, E. P. G.; Bögels, G.; Arkenbout, G. J. *J. Cryst. Growth* **1998**, *191*, 169−177). It was calculated that the incorporation of cyclohexanol into ϵ-caprolactam would be most significant for the {110} form and that the extent of partitioning of cyclohexane into the most important growth forms is 10−100 times smaller than those in the cases of cyclohexanol and cyclohexanone. The effect of impurity incorporation on the habit of ϵ-caprolactam crystals was calculated from the modified attachment energies.

1. Introduction

The industrial-scale crystallization of ϵ-caprolactam, the precursor for the important commodity material nylon-6, represents an important step in determining the purity of the end product. Upstream one of the synthetic routes that have been employed, see Figure 1, in the manufacturing process involves a number of steps all yielding side products which, potentially, are deleterious to the performance of the material finally produced. In particular, such heteroimpurities can result in chain termination during polymerization, leading to a wider molecular weight distribution for the resulting polymer. A key step in the synthesis involves the oxidation of cyclohexane to form, successively, cyclohexanol and cyclohexanone. Because of their similarity to caprolactam in terms of molecular structure, these intermediates are known to affect the crystallization of the final caprolactam end product.

Molecular and solid-state modeling techniques have been used to examine the binding energetics for the heterospecies together with the surface properties and crystal habit of the "as-grown" caprolactam crystals. The aim of the study reported here was to examine the integration of cyclohexane, cyclohexanol, and cyclohexanone molecules into caprolactam crystals and to predict their influence on the morphology of the resulting crystals. In addition, a new approach was taken to the problem of solvent influence on the morphology of caprolactam, based on the assumption that the proportion of the imino-tautomeric form of caprolactam in solution is intrinsically solvent dependent and that its presence can, potentially, modify the morphology of caprolatam crystals. It should be noted that while no experiments were carried out to quantify the proportion of the imino-tautomeric form in solutions with different solvents, the presence of this form was assumed to be significant enough to lead to habit modification. Given this hypothesis, the influence of the imino-tautomer of caprolactam (i.e., caprolactim) was modeled using the same tools as employed in the study of the impurities cyclohexane, cyclohexanol, and cyclohexanone.

* To whom correspondence may be addressed. E-mail: r.b.hammond@leeds.ac.uk.

[†] Present address: SSCI Inc., 3065 Kent Ave., West Lafayette, IN 47906-1076, U.S.A.

10.1021/jp034350u CCC: $25.00
Published on Web 11/07/2003

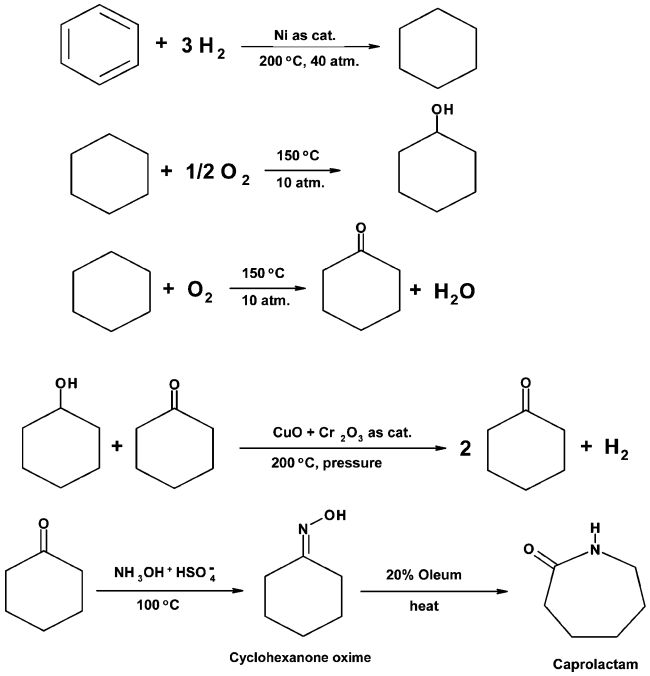

Figure 1. Process for making caprolactam precursor for nylon manufacture: (a, top) hydrogenation of benzene to make cyclohexane; (b, middle top) reaction of cyclohexane to make cyclohexanol and cyclohexanone; (c, middle bottom) reaction of cyclohexanol and cyclohexanone to form pure cyclohexanone; (d, bottom) conversion of cyclohexanone to cyclohexanone oxime followed by a ring opening to make caprolactam.

It is well known that in growth from solutions, the morphology exhibited by the crystals of organic, molecular materials is frequently solvent dependent. It is therefore reasonable to draw a parallel between the mode of action of solute impurities, present in a growth solution, in modifying a crystal habit and that of solvent molecules. Following the development of a methodology for predicting the morphology of pure crystalline phases, as implemented in the computer program HABIT,[1] attention was initially focused on the effects of tailor-made additives on the morphology of host systems. Two categories of additive molecule were envisaged: additives smaller or of the same size as the host that disrupt growth layers[2] and additives larger than the host molecule that block the growth of subsequent layers in the crystal.[3,4] The concepts were later realized as a quantitative approach in the program HABIT95,[5,6] and the overall approach was reviewed.[7]

In the more general case of the impact of growth solvent on the morphology of materials, and here specifically the morphology of ϵ-caprolactam, the impurity molecule is not tailored to the host and, hence, the mode of incorporation into the host lattice is less straightforward to envisage. In a previous theoretical study,[8] a molecular dynamical approach was adopted to investigate the interactions between solvent or solute, impurity molecules, and the most important crystallographic faces in the habit of ϵ-caprolactam. A Monte Carlo approach was also employed to study this system.[9] The molecular dynamical approach allowed a semiquantitative differential binding energy to be evaluated based on the difference in potential energy between the lowest potential energy that could be found for an isolated impurity molecule in contact with an unrelaxed crystallographic surface and the lowest potential energy of an isolated host molecule on the same surface. On crystal surfaces for which a negative differential binding energy was found, this was taken to indicate preferential binding of an impurity molecule in comparison to a host ϵ-caprolactam molecule and hence an increase in the morphological importance of that face due to reduction in the growth rate. A linear scaling factor (albeit arbitrary in terms of absolute magnitude) was derived from the differential binding energies and was used to adjust the relative growth rates of the significant crystal surfaces in the growth habit, predicted from attachment energy calculations, and hence to calculate modified crystal morphologies for ϵ-caprolactam for the growth solvents of interest. Although the approach gave significant insight into the modification of the crystal habit of ϵ-caprolactam, the physical model that was assumed is incomplete in that it does not fully take account of the effects on the crystal lattice and hence on the deposition of subsequent growth layers of the incorporation of an impurity molecule within the host lattice.

However, in the case of additives falling into the category of crystal-growth blockers, it had been identified that the original approach to additive-mode calculations within HABIT95 was hampered by the rigid-fit procedure employed for locating an additive molecule within the host crystal lattice. The fitting procedure overlaid, exactly, some common moiety of the additive and host molecule. Recently, a new development in the methodology[10] has enabled the positions of additive molecules to be optimized, within the context of a host crystal lattice, through minimization of the cohesive energy of the system with respect to the position and orientation of the additive molecule. Hence, given that optimal positions of additive molecules within the host lattice are now identified, these configurations can be evaluated, realistically, using the existing protocols in HABIT95. A successful application of the approach was made treating a number of simple, polyaromatic hydrocarbon binary systems, for example, biphenyl, as an additive in phenanthrene.[10] A further extension of the approach is reported here that allows the treatment of more challenging systems in which specific, hydrogen-bonding interactions play an important role in the crystal packing, in this case, ϵ-caprolactam modeled in the presence of cyclohexane, cyclohexanol, cyclohexanone, and caprolactim. The new development addresses the fact that, given highly directed intermolecular forces associated with hydrogen bonding, there is a much greater risk of locating positions for the additive molecule that are local rather than global minima in terms of lattice energy. An additional protocol employed in selecting the location of the heteromolecule is described that is designed to ameliorate the problem leading, we believe, to a more robust method. Attractively, the approach is also used to provide semiquantitative estimates of impurity segregation coefficients.

2. Theoretical Background and Computational Methodology

The molecular geometry of caprolactam was taken from a single-crystal structure determination.[11] ϵ-Caprolactam crystallizes with a monoclinic unit cell: $a = 19.28$ Å, $b = 7.78$ Å, $c = 9.57$ Å, and $\beta = 112.39°$ in space group $C2/c$ with eight molecules in the unit cell. Initial molecular models for cyclohexane, cyclohexanol, cyclohexanone, and caprolactim were built using the known atomic connectivities and standard bond lengths and bond angles within the Cerius[2] molecular modeling package[12] and then optimized using the semiempirical methods MNDO,[13] AM1,[14] and PM3[15] within the program MOPAC.[16] Geometry optimizations were carried out using the Eigen-vector following method. Optimum structures obtained initially were further optimized specifying the keyword PRECISE, thus decreasing the convergence criteria by a factor of 100. For the

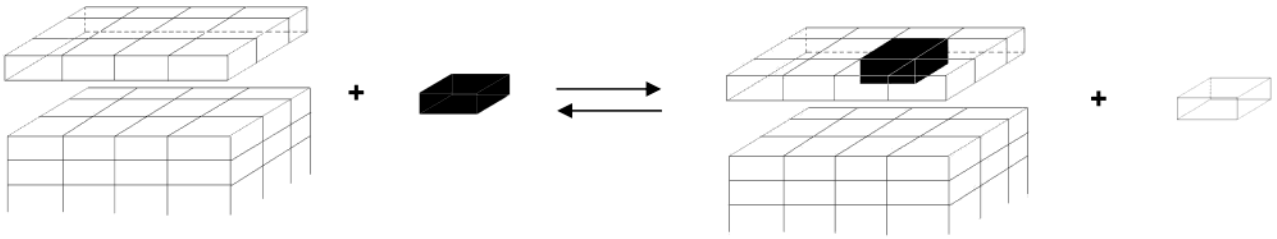

Figure 2. Schematic illustrating the concept of an equilibrium between a pure growth slice and an impurity-containing growth slice attaching to the surface of a pure crystal. The solid blocks represent impurity molecules and the clear blocks host molecules.

purpose of comparison, geometry optimizations using these methods were also performed on caprolactam using the molecule from the single-crystal structure as the starting point. Since, in all cases, the optimized molecular geometries derived using the three different methods were found to be in close agreement, the AM1 derived geometries were selected for use in all subsequent calculations.

Crystal lattice E_{cr}, slice E_{sl}, and attachment E_{att} energies were calculated using an atom−atom approach to evaluate the nonbonded interactions within the bulk crystal. The surface attachment energy, E_{att}, is defined as the energy released when a crystallographically ordered layer (defined by Miller indices (*hkl*)) is incorporated into a bulk crystal. Accordingly, the lattice energy is the sum of the slice and attachment energies

$$E_{cr} = E_{sl}^{hkl} + E_{att}^{hkl} \tag{1}$$

It has been demonstrated that, for a variety of growth mechanisms, growth rates normal to crystal surfaces are proportional to the associated surface attachment energies[17] and in particular that for two-dimensional growth mechanisms the proportionality is linear to a good approximation. Hence calculated attachment energies can be used as a measure of the growth rate of the individual growth forms present as crystal surfaces. Combining all faces provides a route to predict the growth morphology. A model morphology is obtained using a classical Gibbs-Wulff polar plot[18] by assuming that E_{att} is directly proportional to the center−face distance in a crystal as grown. The slowest-growing faces (those with the lowest E_{att} values) are not faceted out and therefore dominate the final crystal morphology at the expense of the smaller, fast-growing faces (high E_{att}).

The likelihood of impurity incorporation on a particular crystal surface (*hkl*) was estimated by calculating the differential binding energy, Δb, between an impurity molecule interacting with the host crystal on that surface and a host molecule interacting with the host crystal. Hence, the differential binding energy is given by

$$\Delta b = E'_{sl} - E_{sl} - \Delta E_{att}^{UVWZ} \tag{2}$$

The term E'_{sl} is the slice energy evaluated by substituting an impurity molecule for a host molecule as the central, referencing molecule and is averaged over all space-group symmetry-related positions in one unit cell. The term ΔE_{att}^{UVWZ} is the difference in the molecule−molecule interaction energy between a central host molecule, within the slice, and the closest host molecule (based on the center−center distance to an adjoining position referenced by multiples *U*, *V*, and *W* of the unit cell along the crystal directions and the symmetry position *Z*) outside the slice and an impurity molecule substituted at the same lattice position outside the slice. Further, modified attachment energies, E''_{att}, are defined as the energy released, from the perspective of the impurity molecule, when a slice having an impurity molecule as the central molecule is incorporated within a pure host crystal. Calculations of Δb values and modified attachment energies E''_{att} for each morphologically important face were performed using the HABIT95 program in additive mode. Two submodes of the additive mode are available, depending on the size and effect of the impurity within the host crystal lattice:

(1) A disrupter mode for impurities of the same size, or smaller, than a molecule of the host crystal. This mode does not allow any vacancy near the impurity when performing the attachment energy calculations.

(2) A blocker mode for impurities larger than the molecules of the host crystal or in a position necessitating vacancies around the impurity, allowed in this mode, for growth to resume.

The approach for calculating differential binding energies and modified attachment energies, as described so far, has been extended through the development of a lattice-energy minimization module, described in full below, that allows the position of an impurity molecule to be relaxed within the context of the host crystal lattice.

The equilibrium impurity-segregation coefficient, K_p, for solidification in liquid/solid systems is given by eq 3, where $[X]_S$ and $[X]_L$ are the concentrations of the impurity species in, respectively, the solid and liquid phases

$$K_p = \frac{[X]_S}{[X]_L} \tag{3}$$

For a simple equilibrium A ↔ B, from statistical thermodynamics, we can write the following expression, eq 4, for the associated equilibrium constant *K*

$$K = \frac{z_B}{z_A} \exp\left(\frac{-\Delta\epsilon_0}{\kappa T}\right) \tag{4}$$

Here, z_A and z_B are the molecular partition functions of species A and B, $\Delta\epsilon_0$ is the difference between the ground-state energy levels, κ is the Boltzmann constant, and *T* is the absolute temperature. Hence, the difference in internal energy between the two states A and B at 0 K, ΔU_0, is equal to $N_a\Delta\epsilon_0$ where N_a is Avogadro's number. The physical process underpinning the incorporation of an impurity molecule into the host solid can be regarded as analogous to such an equilibrium A ↔ B, and this idea is illustrated schematically in Figure 2. If it is assumed that there is a negligible internal energy difference between an impurity molecule and a host molecule in the liquid phase, ideal behavior, then the calculated differential binding energy Δb can be equated with the overall internal energy change ΔU_0 associated with the incorporation of an impurity molecule into the host crystal surface. This approximation is, potentially, less justifiable for solidification from the melt but rather better when the liquid is a dilute solution phase. If it is further assumed that the temperature dependences of these energy differences are small and that the molecular partition functions z_A and z_B can be equated, then we arrive at the following approximate

expression, eq 5, for the equilibrium impurity segregation coefficient K_p

$$K_p \approx \exp\left(\frac{-\Delta b}{RT}\right) \quad (5)$$

Hence, it is possible using this approach to estimate bulk impurity segregation coefficients by employing an appropriate averaging of the Δb values calculated for individual crystal surfaces.

In this study, the calculations employed the potential parameters due to Momany et al.[19] This potential is of the Lennard-Jones 6-12 type and incorporates, therefore, solely two-body interactions. A separate 10-12 term is included in the potential for treating atoms involved in hydrogen bonding, which can, potentially, be manifested by all the molecules, other than cyclohexane, considered in this study. It was convenient to apply this potential set as no terms involving three atom centers are required for the treatment of hydrogen-bonding interactions. A lattice energy was calculated for the host ϵ-caprolactam crystal. An electrostatic energy contribution was included in this calculation. This employed the atomic point charges derived, by Mulliken population analysis, in a semiempirical molecular orbital calculation, using the AM1 method, on an isolated caprolactam molecule. Attachment energies for the most likely growth forms (initially identified via geometric considerations, i.e., BFDH theory[20]) were calculated for the host system; see also ref 8.

Impurity molecules were fitted into the host crystal lattice in such a way that one impurity molecule replaced one caprolactam molecule in a single unit cell located at the origin of the fractional coordinate system. To determine the initial location of an impurity molecule within the host unit cell, an impurity molecule was superimposed on a host molecule. This procedure was carried out by minimizing the root mean square (rms) difference between the coordinates of three or more corresponding atoms of the molecules using a routine[21] implemented within Interchem-PC.[22] In this study, the structural similarity between the host and impurity molecules meant that it was straightforward to define appropriate pairs of corresponding atoms. The lattice energy of each fitted impurity molecule, in the context of the host lattice, was calculated using the fractional atomic coordinates derived from the fitting procedure. The host molecule over which the impurity molecule was positioned was, of course, neglected in the lattice, slice, and attachment energy calculations. Binding energies and modified attachment energies were calculated for these fitted, but unrelaxed, positions of the impurity molecules.

Subsequently, impurity molecules were optimized in terms of minimizing the calculated lattice energy. Throughout the minimization procedure, the position and orientation of an impurity molecule, treated as a rigid body, were allowed to vary whereas the positions and orientations of all the host molecules were kept fixed. There is, potentially, a risk that the minimization process might locate a local minimum in the calculated lattice energy of the impurity molecule rather than the global minimum. To assess this possibility, the following procedure was adopted. The center of coordinates of the impurity molecule that was derived from the impurity-on-host fitting procedure was used to define a center for rotation. Rotation angles to apply about the three Cartesian axes were specified in the following ranges: $-180° \le \theta_x < 180°$, $-180° \le \theta_y < 180°$, $0° \le \theta_z < 180°$ with a step size of 60°. This defined a coarse, three-dimensional grid with 108 points in the rotational space of the impurity molecule (treated as a rigid body). To locate each point on the grid, the requisite rotations were applied to the atomic Cartesian coordinates of the additive molecule as derived from the rms fitting routine. Lattice energy minimization was then carried out starting from each location on the grid. The calculated lattice energies were then ranked from the lowest (most stable) to the highest (least stable). In instances in which the same minimum was located multiple times, an examination of the corresponding starting positions allowed the range of attraction to the minimum in the parameter space defined by θ_x, θ_y, and θ_z to be determined. In this way, it was possible to assess the level of confidence with which the minimum having the lowest lattice energy could be taken as being the global minimum.

The "global" optimum position of each impurity molecule was used in subsequent calculations. Modified binding and attachment energies were calculated for each impurity within the context of the host crystal lattice. The modified attachment energies were employed to calculate the relative rates of growth of the morphological forms. Models of the resulting crystal morphologies were produced using the computer program SHAPE.[23]

TABLE 1: Heats of Formation Derived Using Three Semiempirical Methods for Fully Optimized, in Vacuo, Molecular Structures of the Impurity Molecules Considered in This Study

	ΔH_f (kcal/mol)		
compound	AM1	PM3	MNDO
cyclohexane	−38.54	−31.03	−34.76
cyclohexanol	−83.47	−72.84	−74.76
cyclohexanone	−63.33	−60.16	−60.11
caprolactim	−51.43	−52.33	−56.25

TABLE 2: Heats of Formation Derived Using Three Semiempirical Methods for an in Vacuo Caprolactam Molecule As Taken from a Single Crystal Structure Determination

degree of geometry optimization of the caprolactam molecule from single crystal study	ΔH_f (kcal/mol)		
	AM1	PM3	MNDO
all atoms unoptimized	−26.78	−31.15	−18.29
hydrogen atoms optimized	−56.99	−52.59	−48.05
all atoms optimized	−60.53	−57.53	−55.38

3. Results and Discussion

3.1. Semiempirical Molecular Orbital Calculations. The calculated standard enthalpies of formation of the impurity molecules considered in this study are summarized, for the three methods employed, in Table 1. Discrepancies as great as 10.6 kcal/mol, as in the case of cyclohexanol using AM1 and PM3, are observed between the heats of formation calculated by different methods. However, the optimized molecular geometries that were located, for a given molecule, using the three different methods are very similar in all cases. The standard enthalpy of formation calculated for the caprolactam molecule taken from the single crystal structure was found to be, approximately, 30 kcal/mol less exothermic than that calculated for the fully optimized molecule. This was found to be mostly due to the positioning of the hydrogen atoms in the single crystal structure as reflected in the heats of formation of the partially optimized molecule presented in Table 2. The changes in the molecular geometry of caprolactam accompanying optimization were, however, slight, and consequently the unmodified molecular structure from the single crystal study was employed in all the subsequent calculations.

3.2. Validation of the Model Force Field. The potential parameters employed in this study were derived from analysis

TABLE 3: Lattice Energies and Their Component Contributions Calculated for Impurity Molecules within the ϵ-Caprolactam Crystal Lattice for the Positions Located (i) by Geometric Fitting, (ii) by Optimization Starting from the Fitted Position, and (iii) by Grid-Search Optimization (Global Minimum)[a]

lattice energy component (kcal/mol)	cyclohexane			cyclohexanol			cyclohexanone			caprolactim		
	initial	initial optimized	global optimum	initial	initial optimized	global optimum	initial	initial optimized	global optimum	initial	initial optimized	global optimum
total	−2.30	−9.84	−9.84	12.12	−8.51	−12.73	−11.13	−12.47	−12.47	760.26	−8.68	−12.35
van der Waals r^{-6}	−19.28	−18.17	−18.17	−21.90	−20.81	−20.33	−19.79	−19.51	−19.51	−32.53	−23.09	−23.50
van der Waals r^{-12}	16.94	8.33	8.33	34.28	11.88	10.91	9.90	8.51	8.51	793.17	14.54	14.94
HB[b] van der Waals r^{-10}	n/a	n/a	n/a	−0.29	−0.093	−12.15	−3.54	−4.06	−4.06	−3.98	−0.13	−14.20
HB van der Waals r^{-12}	n/a	n/a	n/a	0.12	0.031	9.34	2.98	3.53	3.53	3.00	0.051	11.24
Coulombic	0.034	0.000	0.000	−0.09	0.48	−0.51	−0.68	−0.93	−0.93	0.59	−0.039	−0.83

[a] For comparison, the values [kcal/mol] for the host lattice are total, −16.46; van der Waals r^{-6}, −22.28; van der Waals r^{-12}, 9.41; HB van der Waals r^{-10}, −9.15; van der Waals r^{-12}, 8.02; and Coulombic, −2.46. [b] HB ≡ hydrogen bonding.

of the experimentally determined crystal structures of several hydrocarbons, carboxylic acids, amines, and amides. Hence, it was anticipated that these parameters would be suitable to treat both the host and additive molecules selected for study. To test this hypothesis, it is useful to compare the calculated lattice energy for the host crystal with the reported sublimation enthalpy of ϵ-caprolactam. Two independently determined values for the sublimation enthalpy are reported, first[24] 20.6 ± 0.2 kcal/mol at 338 K and second[25] 20.8 ± 0.1 kcal/mol at 342 K (calculated as the sum of the enthalpy of melting and enthalpy of vaporization at 342 K). The calculated lattice energy, Table 3, is −16.5 kcal/mol for the reported crystal structure. When the crystal structure is optimized (including relaxation of the appropriate unit cell parameters), treating the caprolactam molecules as rigid bodies, the calculated lattice energy reduces to −17.3 kcal/mol. The rms change in the reciprocal cell parameters **a***, **b***, and **c*** on lattice optimization is 2.32%.

Although use of the Momany force field parameters leads to an underestimation of the absolute magnitude of the lattice energy, it should be noted that the value of the dielectric constant stipulated for the calculation of the electrostatic component of the lattice energy is 2. For comparison, using the Dreiding force field parameters,[26] the calculated lattice energy of the crystal structure, optimized with that force field, is −19.1 kcal/mol; however, the van der Waals energy term contributes −14.7 kcal/mol compared with −15.0 kcal/mol for the Momany force field. The difference lies in the choice of a dielectric constant of unity for the electrostatic energy term for the Dreiding force field calculation. It should be noted that in deriving the force-field parameters, Momany et al. employed the semiempirical method CNDO/2 (a choice that is no longer practical) to calculate atomic monopole charges rather than the AM1 method used here. Not withstanding this, the performance of the Momany force field was considered to be satisfactory in terms of both the calculated lattice energy and the small change observed in the lattice constants accompanying structural relaxation. A recent examination[27] of the sensitivity of crystal-morphology predictions to the choice of model intermolecular potential has demonstrated that using normalized attachment energies, as a measure of relative growth rate, yields model morphologies that vary only slightly with the choice of force-field parameters.

3.3. Optimization of the Position of Impurity Molecules within the Host Lattice. A set of five carbon atoms, and the ten hydrogen atoms bonded to them, that specifically excluded any carbon atom bonded to oxygen was taken to define the corresponding atoms that were used to calculate the best geometric fit between each impurity molecule and a host caprolactam molecule. Hence, by application of this protocol, only in the case of cyclohexane was there any choice in the subset of atoms to use and here all the choices were equivalent. The lattice energies calculated for each impurity molecule located in the initial, geometrically fitted position within the host caprolactam lattice are given in Table 3. Table 3 also details the calculated lattice energy for the optimized position of each impurity molecule, where the starting point for the optimization was the fitted position, and the "global" minimum in lattice energy found in the grid search procedure using a grid centered on the same fitted position. In Figure 3, the orientation and position of the impurity molecules, in their global minimum-energy configuration, is illustrated with respect to the host molecule with which the impurity was originally matched.

In all cases except cyclohexanone, there is a substantial reduction in the lattice energy calculated for the impurity molecule when its location and orientation are allowed to relax, via rigid body translations and rotations, from the position found by fitting on the basis of molecular geometry. Further, the minimum lattice energy configuration located in the cases of cyclohexanol and caprolactim was found to be a local minimum. After all the minima in lattice energy found in the grid optimization procedure were ranked, and identical minima were clustered, i.e., the same minima but located from different starting positions, the lowest lattice energy obtained was taken to indicate the global optimum position of the impurity molecule in the ϵ-caprolactam lattice. Accordingly, improved locations were identified for cyclohexanol and caprolactim impurities. In both cases, optimization starting from the position identified by fitting the molecular geometries failed to locate configurations in which the impurity molecule forms a hydrogen-bonded interaction with a host molecule. Whereas a different choice of corresponding atoms in the fitting procedure may have been sufficient to circumvent the problem of locating a local minimum, it is particularly useful that the necessity for this level of user intervention has been removed by employing a grid-search approach for locating energy minima. The approach permits considerable confidence that the positions thereby located for the impurity molecules are indeed global minima in terms of calculated lattice energy.

The results of clustering the minima found in the grid-search procedure in terms of optimized lattice energy, summarized in Table 4, suggest that the problem of multiple minima is particularly manifested when the impurity molecule can form specific hydrogen-bonded interactions with a molecule in the host lattice. Conversely where the intermolecular interactions are roughly isotropic the problem is largely absent, as demonstrated in the case of cyclohexane here and hence, by inference, also in the case of a recent study of the segregation of biphenyl into solid naphthalene and phenanthrene and anthracene into solid phenanthrene.[10] Taking these global optimum positions for the impurity molecules in the host lattice, in all cases it was found that no vacancies were then required (i.e., the neglecting of additional host molecules in the lattice energy summations due to overlap between the impurity molecule and those specific

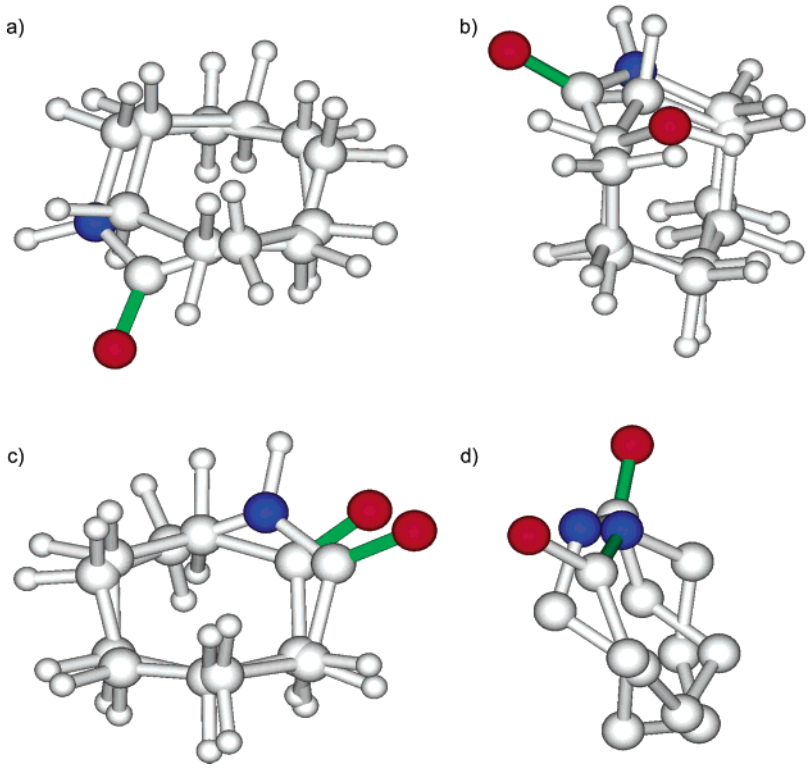

Figure 3. Overlay of the optimized position of each impurity molecule in the context of the ϵ-caprolactam lattice with a host molecule at the equivalent lattice position for (a) cyclohexane, (b) cyclohexanol, (c) cyclohexanone, and (d) caprolactim (hydrogen atoms omitted for clarity). Oxygen atoms are colored red, nitrogen atoms are blue, and double bonds are green.

TABLE 4: Ranked Energy Minima (Energy < 0.0 kcal/mol) Found for Impurity Molecules in the Grid-Search Minimization Procedure with Associated Cluster Sizes (i.e., the number of starting locations from which the same minima was located)

	cyclohexane		cyclohexanol		cyclohexanone		caprolactim	
rank of cluster	cluster energy (kcal/mol)	no. of starting positions in cluster	cluster energy (kcal/mol)	no. of starting positions in cluster	cluster energy (kcal/mol)	no. of starting positions in cluster	cluster energy (kcal/mol)	no. of starting positions in cluster
1	−9.84	42	−12.73	6	−12.47	6	−12.35	12
2	−9.33	22	−12.03	6	−11.61	7	−12.01	6
3	−9.18	23	−10.72	13	−11.35	10	−11.42	2
4	−4.90	3	−10.43	8	−11.08	4	−10.57	3
5	−2.36	2	−10.37	3	−10.96	11	−9.42	12
6	−2.16	2	−9.96	4	−10.78	7	−8.68	7
7	−0.70	6	−9.70	6	−10.43	2	−8.27	5
8			−9.67	10	−10.33	5	−8.20	4
9			−8.88	9	−10.14	13	−8.19	4
10			−8.51	5	−9.89	7	−7.80	4

host molecules) in the additive mode calculations of differential binding energies and modified attachment energies performed using HABIT95.

3.4. Disruption of the Intermolecular Hydrogen Bonding on Incorporation of Impurity Molecules. In the ϵ-caprolactam crystal structure, pairs of molecules are associated as dimers connected by two strong hydrogen bonds. The two molecules in a dimer are related by a combination of the inversion symmetry element with the C center of the monoclinic lattice. There are no further hydrogen-bonded interactions between adjacent dimers. As a consequence, it is inevitable that the incorporation of an impurity molecule into the caprolactam lattice will involve the loss of two strong hydrogen bonds for a host molecule. The corresponding loss in intermolecular bonding energy may be partially offset through the formation of hydrogen-bonded interactions between host and impurity molecules where this is chemically possible. Clearly, cyclohexane cannot form any substitute hydrogen bonds on replacing a host molecule in the lattice. The other impurity molecules have the potential to form hydrogen bonds, and all do so (see Table 3), as manifested in the most stable configuration of the impurity within the caprolactam lattice although, in the case of cyclohexanone, the hydrogen bonded interactions are weak 0.54 kcal/mol (cf. 2.81 and 2.96 kcal/mol for cyclohexanol and caprolactim, respectively).

The optimal positions of the impurity molecules cyclohexanol, cyclohexanone, and caprolactim in the context of the ϵ-caprolactam host lattice are illustrated in Figure 4. In each case, the carbon atoms of the impurity molecule are colored green, those of the substituted caprolactam molecule are colored magenta, and those of the caprolactam molecule for which the hydrogen-bonded interactions are missing are colored orange. The hydrogen bonds that are broken on substitution of an impurity molecule for a host molecule are indicated by red arrows and those that are formed are indicated by green arrows. In the case of cyclohexanol, the most favorable arrangement found has the hydroxyl group forming a hydrogen bond with an oxygen atom of an adjacent, complete caprolactam dimer; hence one host

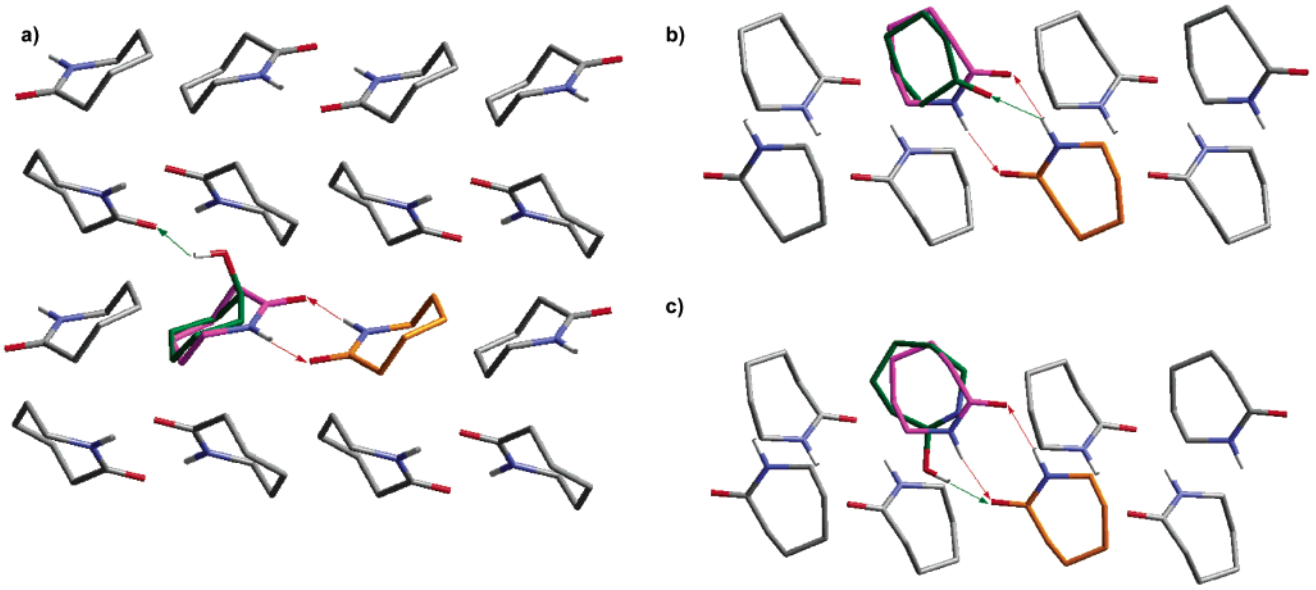

Figure 4. Optimal position of the impurity molecules (a) cyclohexanol, (b) cyclohexanone, and (c) caprolactim in the ϵ-caprolactam host lattice. Carbon atoms of the impurity molecule are colored green, those of the substituted caprolactam molecule are magenta, and those of the caprolactam molecule, for which the hydrogen-bonded interactions are missing, are orange. The hydrogen bonds that are broken on substitution of an impurity molecule for a host molecule are indicated by red arrows. Hydrogen bonds that formed are indicated by a green arrow.

molecule remains uncompensated in terms of two broken hydrogen bonds. In contrast to this, cyclohexanone and caprolactim molecules are incorporated most favorably in such a way that the host molecule, for which two hydrogen bonds are lost in the substitution, now forms one compensating hydrogen bond with the impurity molecule. Note that the ring nitrogen of the caprolactim molecule is too far, 2.9 Å, from the amino hydrogen of the caprolactam molecule for there to be considered a hydrogen-bonded interaction present. In consideration of the foregoing discussion, it should be borne in mind that, currently, at this stage in its development the methodology does not allow for the local perturbation of the host structure in response to the disturbance in the crystal field caused by the presence of the impurity molecule.

3.5. Segregation of Synthesis Impurities in Solid ϵ-Caprolactam and Impact of Impurities on Crystal Morphology. When grown from the vapor phase, ϵ-caprolactam has a hexagonal-plate morphology with dominant {200} forms bounded by {110} and {11$\bar{1}$} forms.[28] When grown from alcohols, ethyl acetate, propanone, toluene, and water under conditions of low supersaturation, the {31$\bar{1}$} form is also found in the final morphology.[29] In contrast, crystals grown from *n*-alkanes are thin plates with {200} faces probably bounded by {111} faces. Other theoretical calculations of the morphology of pure ϵ-caprolactam appear in the literature.[30] There is an issue considered in both experimental and theoretical treaties as to whether the fundamental growth unit for caprolactam is a single molecule or a hydrogen-bonded dimer. It is suggested[30] that dimers are prevalent in aprotic, nonpolar solvents whereas monomers are more likely in polar solvents, especially water. The impact of water on the melt crystallization of ϵ-caprolactam has been studied[31,32] as this is another important impurity that affects the performance of the resulting crystalline product but, more particularly, because melt crystallization as a route for purification is greatly preferable to the existing, energy-intensive, multistage distillation process for the purification of caprolactam. The effect of cyclohexanone as an impurity has also been studied.[33−35]

In this paper, mindful that we are considering both polar and nonpolar impurity species and that the available experimental measurements of segregation coefficients are for melt growth, a justification is required of the implicit assumption, in the calculations that are described, of crystal growth from monomeric units. There were a number of alternative modeling approaches to the question of monomeric vs dimeric growth. Of the impurity molecules considered, only caprolactim is capable of forming a hydrogen-bonded dimer with itself (a structure effectively equivalent to a caprolactam dimer). Hence direct substitution of a host dimer by an impurity dimer is not generally applicable under the assumption that the host crystal grows by addition of dimers. Another possibility was to create an absence of one host molecule in the lattice by substitution of a host dimer with a single impurity molecule. However, in the cases of the impurity molecules cyclohexanone and caprolactim, comparison of the intermolecular pair energies of caprolactam molecule with impurity molecule pairs and host dimers showed that the energies are very similar in the case of caprolactim and, although the pair energy for caprolactam-cyclohexanone is ~2 kcal/mol less favorable, this pseudodimer still makes the largest single, most favorable contribution to the lattice energy summation decomposed over individual molecule−molecule pairs. The pair energy values are for a host dimer, −3.64 kcal/mol; for a cyclohexanone−caprolactam pair, −1.58 kcal/mol; and for a caprolactim−caprolactam pair, −3.56 kcal/mol. Given this, it seemed reasonable, for all the impurity species, to treat the case in which one host molecule is substituted by an impurity molecule. A more complex scenario in which a host dimer is substituted by two independent impurity molecules is the subject of ongoing investigation. In the following sections, the results of the current study for the individual impurity species are presented.

3.5.1. Cyclohexane. The calculated values of the differential binding energies for the important growth forms {200}, {110}, and {11$\bar{1}$}, given in Table 5, suggest that cyclohexane is unlikely to partition into these growth slices to any great extent. By use of eq 5, the calculated equilibrium segregation coefficients at 298 K are 2.4×10^{-5} for the (200) slice, 1.5×10^{-4} for the (110) slice, and 3.0×10^{-4} for the (11$\bar{1}$) slice. It is interesting to try and rationalize why ϵ-caprolactam crystallizes from the alkanes as flat plates dominated by the {200} form.[29] In the

TABLE 5: Differential Binding Energies, Attachment Energies, and Relative Growth Rates Calculated for the Impurity Cyclohexane on the Crystallographically Most Important Faces of ϵ-Caprolactam[a]

growth face	differential binding energy Δb (kcal/mol)		AE for host onto impurity-containing slice E''_{att} (kcal/mol)		AE for host on pure-host slice E_{att} (kcal/mol)	relative growth rates scaled on AE of (200) face		
	fitted	optimized	fitted	optimized		fitted	optimized	pure host
(200)	8.85	6.31	−2.85	−3.71	−4.01	1.00	1.00	1.00
(110)	6.90	5.20	−2.29	−3.98	−5.33	0.80	1.07	1.33
(11$\bar{1}$)	6.55	4.81	−3.28	−4.94	−6.68	1.15	1.33	1.67
(111)	4.77	3.33	−4.12	−6.07	−9.30	1.45	1.64	2.32
(31$\bar{1}$)	6.07	4.15	−4.01	−5.48	−7.88	1.41	1.48	1.97
(20$\bar{2}$)	4.18	2.33	−5.27	−6.82	−11.21	1.85	1.84	2.80
(310)	3.86	3.12	−3.58	−6.24	−9.67	1.26	1.68	2.41
(002)	4.89	2.16	−6.23	−6.90	−11.46	2.19	1.86	2.86
(11$\bar{2}$)	3.07	1.25	−5.31	−6.89	−12.19	1.86	1.86	3.04
(40$\bar{2}$)	3.65	2.67	−4.60	−7.02	−11.07	1.61	1.89	2.76

[a] Values are given for the initial, geometrically fitted position and the position of global minimum in lattice energy.

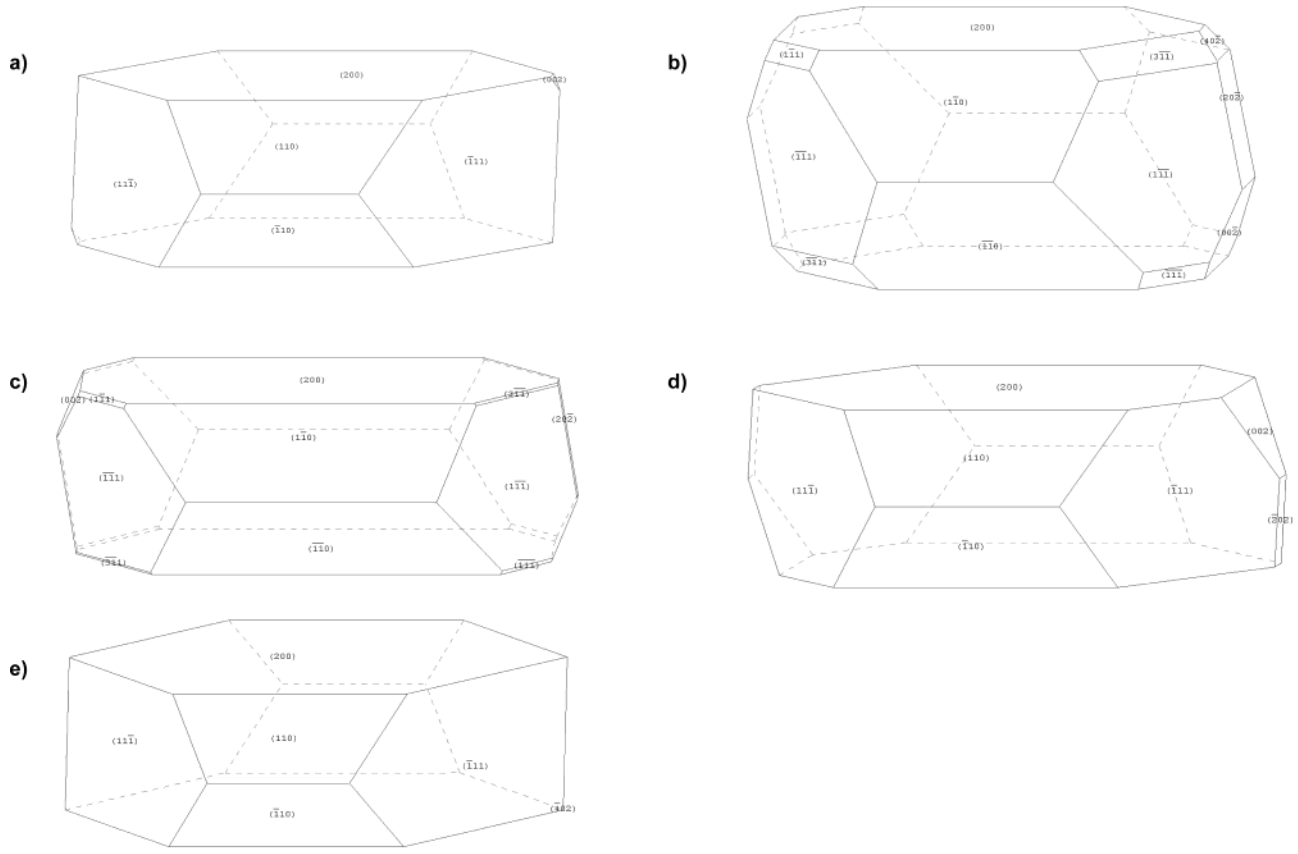

Figure 5. Calculated morphologies for (a) pure ϵ-caprolactam and ϵ-caprolactam in the presence of (b) cyclohexane, (c) cyclohexanol, (d) cyclohexanone, and (e) caprolactim.

present case, although the slice energies for the (200) face calculated from the perspective of a central host and central cyclohexane molecule, E_{sl} and E'_{sl}, are different by 6.3 kcal/mol, the difference in the attachment energies, E_{att} and E''_{att}, is only 0.3 kcal/mol. Herein lies a possible explanation in terms of cyclohexane, which may also be indicative of the general case for the alkanes, namely, that although there is no significant energy barrier to the competitive adsorption of cyclohexane molecules on the (200) crystal surface, completion of a new (200) layer is rendered quite energetically unfavorable, in terms of lattice-site energy, by the presence of cyclohexane molecules. Further the differences between E_{att} and E''_{att} are larger for the (110) and (11$\bar{1}$) faces, 1.4 and 1.7 kcal/mol, respectively, suggesting that adsorption of cyclohexane on these crystal surfaces should be less favorable. In crystallizations of ϵ-caprolactam employing cyclohexane as a solvent rather than in its presence as a trace impurity, an additional factor would be a statistical one in that the concentration of solute is much less than that of the solvent so substantially increasing the solvent's effectiveness in disrupting growth on the (200) surface. In essence, this is the mechanism for controlling the morphology of caprolactam crystallized from alkanes that was previously suggested, qualitatively, by van der Heijden et al.[30]

In consideration of the modified morphology calculated for caprolactam crystals in the presence of cyclohexane, illustrated in Figure 5, it is important to remember that this prediction, based on the modified attachment energies for the faces E''_{att}, does not take into account any destabilizing effects that may occur within the individual growth slices due to the presence of the impurity. Essentially, E''_{att} is a measure of the growth rate normal to the crystal surface expedited by the presence of an impurity molecule at a lattice site in the surface on which growth

TABLE 6: Differential Binding Energies, Attachment Energies, and Relative Growth Rates Calculated for the Impurity Cyclohexanol on the Crystallographically Most Important Faces of ϵ-Caprolactam[a]

growth face	differential binding energy Δb (kcal/mol)		AE for host onto impurity-containing slice E''_{att} (kcal/mol)		AE for host on pure-host slice E_{att} (kcal/mol)	relative growth rates scaled on AE of (200) face	
	fitted	optimized	fitted	optimized		optimized	pure host
(200)	26.53	3.45	−3.02	−3.75	−4.01	1.00	1.00
(110)	7.80	2.26	14.34	−3.98	−5.33	1.06	1.33
(11$\bar{1}$)	15.15	3.30	5.64	−6.36	−6.68	1.70	1.67
(111)	13.57	1.86	4.61	−7.54	−9.30	2.01	2.32
(31$\bar{1}$)	14.80	2.79	4.79	−7.06	−7.88	1.88	1.97
(20$\bar{2}$)	5.47	2.25	10.91	−9.63	−11.21	2.57	2.80
(310)	11.84	1.62	5.97	−7.67	−9.67	2.05	2.41
(002)	7.76	2.00	8.37	−9.64	−11.46	2.57	2.86
(11$\bar{2}$)	8.23	0.58	7.05	−9.16	−12.19	2.44	3.04
(40$\bar{2}$)	3.32	2.69	13.20	−9.93	−11.07	2.65	2.76

[a] Values are given for the initial, geometrically fitted position and the position of global minimum in lattice energy. Relative growth rates are not calculated for the fitted position.

TABLE 7: Differential Binding Energies, Attachment Energies, and Relative Growth Rates Calculated for the Impurity Cyclohexanone on the Crystallographically Most Important Faces of ϵ-Caprolactam[a]

growth face	differential binding energy Δb (kcal/mol)		AE for host onto impurity-containing slice E''_{att} (kcal/mol)		AE for host on pure-host slice E_{att} (kcal/mol)	relative growth rates scaled on AE of (200) face		
	fitted	optimized	fitted	optimized		fitted	optimized	pure host
(200)	4.34	3.07	−2.94	−3.12	−4.01	1.00	1.00	1.00
(110)	4.31	3.25	−4.25	−4.63	−5.33	1.45	1.48	1.33
(11$\bar{1}$)	4.04	3.12	−5.32	−5.84	−6.68	1.81	1.87	1.67
(111)	2.50	1.82	−6.40	−7.15	−9.30	2.18	2.29	2.32
(31$\bar{1}$)	3.70	2.77	−6.19	−6.70	−7.88	2.11	2.15	1.97
(20$\bar{2}$)	2.21	1.62	−7.95	−8.81	−11.21	2.70	2.82	2.80
(310)	2.37	1.81	−6.64	−7.52	−9.67	2.26	2.41	2.41
(002)	1.15	0.76	−7.15	−8.21	−11.46	2.43	2.63	2.86
(11$\bar{2}$)	1.11	0.73	−7.91	−8.96	−12.19	2.69	2.87	3.04
(40$\bar{2}$)	3.41	2.57	−9.02	−9.62	−11.07	3.07	3.08	2.76

[a] Values are given for the initial, geometrically fitted position and the position of global minimum in lattice energy.

is taking place. One must, therefore, make reference to the magnitude of the differential binding energy for each surface when assessing the efficacy of the morphological model. In this case, the modified model predicts a richer morphology with, in addition to those forms manifested by the pure host system, the {111}, {31$\bar{1}$}, {20$\bar{2}$}, and {40$\bar{2}$} forms present.

3.5.2. Cyclohexanol. For the most important growth forms {200}, {110}, and {11$\bar{1}$}, the values of the differential binding energies, reported in Table 6, suggest that incorporation is most likely into faces of the {110} form for which the calculated equilibrium segregation coefficient at 298 K is 0.022. The most significant change predicted in the crystal morphology shown in Figure 5, due to the presence of cyclohexanol, is an increase in the relative surface area of the {110} form. In addition, the forms {111}, {31$\bar{1}$}, and {20$\bar{2}$} are now also predicted to appear in the crystal habit. The combination of a propensity for cyclohexanol to segregate into the faces of the {110} form with the increased importance of this form in the crystal morphology emphasizes the necessity for examining crystal surfaces individually when considering the overall incorporation of impurities into the host crystal. It is interesting to note that a well-developed {110} form has been observed, experimentally, in crystals grown from low molecular weight alcohols.[29]

3.5.3. Cyclohexanone. The differential binding energies for the forms {200}, {110}, and {11$\bar{1}$}, as reported in Table 7, are very similar. In the case of cyclohexanone as an impurity in the growth of ϵ-caprolactam from the melt, experimentally measured segregation coefficients are available for the {110} and {11$\bar{1}$} forms.[34] The value of the equilibrium segregation coefficient calculated for the {110} form at 298 K is 4.2×10^{-3} and at 342 K (the melting point of pure ϵ-caprolactam) is 8.4×10^{-3}. The reported experimental values, which are summarized in Table 8, of the same quantity for three concentrations of cyclohexanone in the melt, 0.10, 5.0, and 30.0 mol %, at undercoolings corresponding to supersaturations of, respectively, 3.3×10^{-3}, 3.3×10^{-3}, and 4.7×10^{-3}, are 1.4×10^{-2}, 7.0×10^{-3}, and 7.7×10^{-3}, in excellent agreement with the calculated value. The value of the equilibrium segregation coefficient calculated for the {11$\bar{1}$} form at 298 K is 5.2×10^{-3} and at 342 K is 1.0×10^{-2}. The reported experimental

TABLE 8: Experimentally Determined Segregation Coefficients for the {110} and {11$\bar{1}$} Forms of Caprolactam Crystals Grown from Melts Containing Cyclohexanone Taken from Van Den Berg et al.[34]

cyclohexanone in melt (mol %)	supersaturation $\times 10^3$ $(\Delta H_m(T_m - T)/RT_m^2)$[a]	segregation coefficient for{110} form $\times 10^2$	segregation coefficient for {11$\bar{1}$} form $\times 10^2$
0.10	1.7	1.4	6.5
	3.3	1.4	4.9
	5.0	7.3	9.0
5.0	3.3	0.70	2.0
	4.1	1.1	3.2
	5.8	1.1	4.4
15.0	3.5[b]	3.7	3.9
	3.5[b]	4.9	2.9
	4.4	4.6	3.1
30.0	4.7	0.77	1.1
	5.6	1.3	1.0

[a] ΔH_m is the heat of fusion; T_m, melting temperature; T, temperature; and R, ideal gas constant. [b] Repeated point.

TABLE 9: Differential Binding Energies, Attachment Energies, and Relative Growth Rates Calculated for the Impurity Caprolactim on the Crystallographically Most Important Faces of ϵ-Caprolactam[a]

growth face	differential binding energy Δb (kcal/mol)	attachment energies E_{att} (kcal/mol)		relative growth rates scaled on AE of (200) face	
		host onto impurity-containing slice	host on pure-host slice	caprolactim	pure host
(200)	2.79	−2.71	−4.01	1.00	1.00
(110)	2.92	−4.20	−5.33	1.55	1.33
(111)	2.35	−4.97	−6.68	1.83	1.67
(11$\bar{1}$)	1.91	−7.15	−9.30	2.64	2.32
(31$\bar{1}$)	1.65	−5.47	−7.88	2.02	1.97
(20$\bar{2}$)	1.53	−8.58	−11.21	3.17	2.80
(310)	1.57	−7.18	−9.67	2.65	2.41
(002)	2.47	−9.76	−11.46	3.60	2.86
(11$\bar{2}$)	1.75	−9.88	−12.19	3.65	3.04
(402)	0.88	−7.79	−11.07	2.87	2.76

[a] Values are given for the position of global minimum in lattice energy only.

values at the same three concentrations of cyclohexanone in the melt given above are, respectively, 6.5×10^{-2}, 2.0×10^{-2}, and 1.1×10^{-2}, hence, also giving excellent agreement with the calculated value (also noting that the measured value for the lowest concentration of impurity in the melt is subject to the greatest experimental uncertainty). The expression used to calculate the equilibrium segregation coefficients, eq 5, is most applicable to a crystal growth regime governed by the birth and spread of two-dimensional layers in which the liquid−solid interfacial region remains close to equilibrium. Van den Berg et al. comment[34] that at the highest levels of supersaturation in the melt for which experiments were performed, they had anticipated larger segregation-coefficient values due to the entrapment of impurity inclusions accompanying a change in the growth mechanism to one involving macrosteps. They concluded that the observation of lower than expected values was due to the migration of such inclusions to the crystal surfaces, after removal of the crystal from the melt, and then loss of cyclohexanone by evaporation from the crystal surfaces. Recently, experimental measurements[35] have been reported for crystals grown by layer melt crystallization from a melt with a composition 95 wt % ϵ-caprolactam, 5 wt % cyclohexanone. The measurements indicate a considerably larger value for the bulk segregation coefficient, but this is due to the inability of cyclohexanone inclusions to migrate away from the interfacial region and thereby to avoid incorporation into the growing crystal. In conclusion, it would seem reasonable to take the calculated segregation-coefficient values as indicating, for a given crystal surface, the greatest degree of separation of an impurity from a desired product that can be achieved by crystallization given the most favorable growth conditions (small undercoolings/supersaturations).

The modified morphology of ϵ-caprolactam in the presence of cyclohexanone, illustrated in Figure 5, is largely unchanged with respect to that predicted for the pure host system. The only difference is the presence of a significant {002} form and the appearance of the {20$\bar{2}$} form. An earlier molecular dynamical study of the interaction between solvent molecules and the important crystal surfaces in the habit of caprolactam[8] indicated that cyclohexanone molecules can locate a very energetically favorable binding site on the {31$\bar{1}$} surfaces. This led to the prediction of substantial {31$\bar{1}$} faces in the crystal morphology of ϵ-caprolactam modified by the presence of cyclohexanone. It is reasonable to conclude that the same change in morphology is not predicted by the current approach because here the position of the cyclohexanone molecule, subsequently used as the basis for the attachment energy calculations, is located by energy optimization within the context of the bulk host lattice rather than by energy optimization of a cyclohexanone molecule on specific crystal surfaces. In the latter case, the phase space available for the cyclohexanone molecule to explore is essentially unrestricted, allowing more energetically favorable positions to be located, while in the former case it is highly restricted.

3.6. Influence of the Imino Tautomeric Form on the Morphology of ϵ-Caprolactam. The predicted impact on the crystal morphology of the presence of the imino tautomeric form of caprolactam, illustrated in Figure 5, is slight given that the effects are roughly isotropic with equivalent reductions of the growth rates normal to each face. At the same time, the differential binding energies on the crystal surfaces, as reported in Table 8, are generally small. Hence, in answer to the initial speculation as to the effect of the presence of caprolactim on the crystallization of caprolactam, it seems likely that the caprolactim species would be incorporated into the host lattice, but at the same time, the impact would be a similar reduction of growth rate on all the crystal surfaces. It is interesting to note that the hydrogen-bonding interactions observed in the optimal arrangement of a caprolactim molecule within the host lattice, Figure 4, exploit only one of the two possible hydrogen-bond donor−acceptor pairings, namely, hydroxyl hydrogen atom−carbonyl oxygen atom. This is, presumably, a result of the packing forces exerted by the surrounding caprolactam molecules which prevent the caprolactim molecule assuming a position in which a hydrogen bond between the amino hydrogen atom and imino nitrogen atom is formed alongside the aforementioned hydrogen bond.

4. Conclusions

A procedure has been developed for identifying the most energetically favorable location and orientation of impurity molecules in host crystals. This builds on well-established protocols, for examining the impact of impurities on the morphology of molecular crystals, that are implemented in the computer program HABIT95. A grid-searching approach has been employed for identifying minima in the calculated lattice energy in an attempt to ensure that the position of the global minimum in lattice energy is located. By use of the optimal configurations identified in these calculations, differential binding energies and modified attachment energies are calculated for the important growth forms, the former values then enable equilibrium segregation coefficients to be calculated for each form.

The approach has been applied to study the impact of three impurities, cyclohexane, cyclohexanol, and cyclohexanone, on

the crystallization of ϵ-caprolactam. It was found that cyclohexane is the impurity least compatible with the host lattice having calculated equilibrium segregation coefficients, for the principal crystal forms, that are between 1 and 2 orders of magnitude smaller than the corresponding values for cyclohexanol and cyclohexanone. This is understandable, given crystal growth from monomer units, since cyclohexane is incapable of participating in hydrogen-bonded interactions. The equilibrium segregation coefficients calculated for the partitioning of cyclohexanone into the {110} and $\{11\bar{1}\}$ forms of ϵ-caprolactam were found to be in excellent agreement with reported experimental values for crystals grown from the melt. In general, the impurities were predicted to lead to an increase in the number of forms present in the crystal habit, and the predicted increase in the relative surface area of the {110} form in the presence of cyclohexanol is of particular significance since this is also the major form that has the largest calculated equilibrium impurity segregation coefficient.

The results of this study are encouraging in the context of developing molecular modeling techniques, with quantitative reliability, for predicting properties of materials that are important for evaluating their behavior under realistic process conditions. In particular, the ability to estimate equilibrium segregation coefficients for particular impurities in specific crystal surfaces is of great significance for evaluating the impact of process conditions on the purity of a resulting product.

Future developments will, among other things, address the refinement of the modeling procedure so that the effect of the local relaxation of the host crystal lattice about the site of an impurity molecule can be taken into account.

Acknowledgment. This work has been funded by EPSRC/ROPA Grant GR/M78052, which the authors gratefully acknowledge. The authors would also like to thank Dr. Matthew J. Jones for providing Figure 1.

References and Notes

(1) Clydesdale, G.; Roberts, K. J.; Docherty, R. *Comput. Phys. Commun.* **1991**, *64*, 311−328.
(2) Clydesdale, G.; Roberts, K. J.; Docherty, R. *J. Cryst. Growth* **1994**, *135*, 331−340.
(3) Clydesdale, G.; Roberts, K. J.; Lewtas, K.; Docherty, R. *J. Cryst. Growth* **1994**, *141*, 443−450.
(4) Clydesdale, G.; Roberts, K. J.; Lewtas, K. *Mol. Cryst. Liq. Cryst.* **1994**, *248*, 243−276.
(5) Clydesdale, G.; Roberts, K. J.; Docherty, R. *J. Cryst. Growth* **1996**, *166*, 78−83.
(6) Clydesdale, G.; Roberts, K. J.; Docherty, R. J. *Quantum Chemistry Program Exchange* **1996**, *16*, 1.
(7) Clydesdale, G.; Roberts, K. J.; Walker, E. M. The Crystal Habit of Molecular Materials: A structural Perspective. In *Molecular Solid State: Theoretical Aspects and Computer Modelling of the Molecular Solid State*; Gavezzotti, A, Ed.; John Wiley and Sons: Chichester, 1997; Vol. 1, pp 203−232.
(8) Walker, E. M.; Roberts, K. J.; Maginn, S. J. *Langmuir* **1998**, *14*, 5620−5630.
(9) Roberts, K. J.; Walker, E. M.; Maginn, S. J. *Mol. Cryst. Liq. Cryst.* **1996**, *279*, 233−240.
(10) Clydesdale, G.; Hammond, R. B.; Roberts, K. J. *J Phys. Chem. B* **2003**, *107*, 4826−4833.
(11) Windler, F. K.; Dunitz, J. D. *Acta Crystallogr*. **1975**, *B31*, 268−269.
(12) *CERIUS*^{2} Molecular Modelling Software for Materials Research by Accelrys, Inc., Princeton, NJ, 2000.
(13) Dewar, M. J. S.; Thiel, W. *J. Am. Chem. Soc.* **1977**, *99*, 4899.
(14) Dewar, M. J. S.; Zoebisch, E. G.; Healy, E. F.; Stewart, J. J. P. *J. Am. Chem. Soc.* **1985**, *107*, 3902.
(15) Stewart, J. J. P. *J. Comput. Chem.* **1989**, *10*, 209.
(16) *MOPAC*, version 6.0; Quantum Chemistry Program Exchange Program No. 455. Creative Arts Building 181, Indiana University, Bloomington, IN 47405.
(17) Hartman, P.; Bennema, P. *J. Cryst. Growth* **1980**, *49*, 145−156.
(18) Wulff, G. *Z. Kristallogr*. **1901**, *34*, 499.
(19) Momany, F. A.; Carruthers, L. M.; McGuire, R. F.; Scheraga, H. A. *J. Phys. Chem*. **1974**, *78*, 1595.
(20) Donnay, J. D. H.; Harker, D. *Am. Mineral*. **1937**, *22*, 446.
(21) Nyburg, S. C. *Acta Crystallogr*. **1974**, *B30*, 25.
(22) Bladon, P. Interchem-PC software Version 3.4, http://www.interprobe.co.uk/inter/interprobe.html, **2002**.
(23) Dowty, E. *Am. Mineral*. **1980**, *65*, 465: SHAPE for Windows Version 6, http://www.shapesoftware.com.
(24) Kabo, G. J.; Kozyro, A. A.; Krouk, V. S.; Sevruk, V. M.; Yursha, I. A.; Simirsky, V. V.; Gogolinsky, V. I. *J. Chem. Thermodyn.* **1992**, *24*, 1−13.
(25) Steele, W. V.; Chirico, R. D.; Knipmeyer, S. E.; Nguyen, A. *J. Chem. Eng. Data* **2002**, *47*, 689−699.
(26) Mayo, S. L.; Olafson, B. D.; Goddard, W. A., III *J. Phys. Chem.* **1990**, *94*, 8897−8909.
(27) Brunsteiner, M.; Price, S. L. *Cryst. Growth Des.* **2001**, *1*, 447−453.
(28) Walker, E. M. Ph.D. Thesis, University of Strathclyde, 1997.
(29) van der Heijden, A. E. D. M.; Geertman, R. M.; Bennema, P. *J. Phys. D: Appl. Phys.* **1991**, *24* 123−126.
(30) Geertman, R. M.; van der Heijden, A. E. D. M. *J. Cryst. Growth* **1992**, *125*, 363−372.
(31) Jansens, P. J.; Langen, Y. H. M.; van de Berg, E. P. G.; Geertman, R. M. *J. Cryst. Growth* **1995**, *155*, 126−134.
(32) Bouropoulos, N. C.; Kontoyannis, C. G.; Koutsoukos, P. G. *J. Cryst. Growth* **1997**, *171*, 538−542.
(33) Geertman, R. M. Ph.D. Thesis, University of Nijmegen, The Netherlands, 1993.
(34) van den Berg, E. P. G.; Bögels, G.; Arkenbout, G. J. *J. Cryst. Growth* **1998**, *191*, 169−177.
(35) Kim, K. J.; Ulrich, J. *J. Cryst. Growth* **2002**, *234*, 551−560.